η^5-Pentamethylcyclopentadienyliridium(III) and -rhodium(III) Labeling of Amino Acids with Aromatic Side Chains – The Importance of Relativistic Effects for the Stability of Cp*Ir^{III} Sandwich Complexes

Diran Agaid Herebian, Claudia S. Schmidt, William S. Sheldrick*, and Christoph van Wüllen

Fakultät für Chemie, Ruhr-Universität Bochum,
D-44780 Bochum, Germany
Fax: (internat.) + 49(0)234/7094-420
E-mail: shel@anachem.ruhr-uni-bochum.de

Received June 26, 1997

Keywords: Iridium / Rhodium / Amino acids / Sandwich complexes / Bioorganometallic chemistry / Relativistic effects

η^5-Pentamethylcyclopentadienyliridium(III) and -rhodium-(III) sandwich complexes of the type [(η^5-Cp*)M(η^6-aa)]-(CF_3SO_3)$_2$ (M = Ir, Rh; **3–14**) containing L-tyrosine, L-tryptophan and L-phenylalanine derivatives (aa) can be prepared by treatment of [(η^5-Cp*)ML_3] (CF_3SO_3)$_2$ [L = thf, $(CH_3)_2CO$, CH_3CN] with the appropriate bioligand in thf for *N*-protected compounds and in CF_3COOH for α-amino acids with unprotected amino groups. Coordination to the Cp*M^{III} fragments stabilizes the ketonic form of the tyrosine aromatic side chains, leading to a marked enhancement in the acidity of the *p*-hydroxy function. The crystal structure of [Cp*Ir(ActyrOMe)] (CF_3SO_3)$_2$ (**3b**, ActyrOMe = *N*-acetyltyrosine methyl ester) confirms a marked distortion towards an η^5-oxohexadienyl coordination mode as may be gauged from the tilting of the *p*-OH plane C13/C14/C15 by no less than θ = 12.9° from that of the remaining ring atoms. Facial isomers are present in an effective 1:1 ratio for all tryptophan derivatives. Whereas the Cp*Ir^{III} sandwich complexes of aromatic α-amino acids are stable in polar solvents, rapid decay is observed for analogous Cp*Rh^{III} complexes of *N*-unprotected derivatives in polar solvents. Comparative nonrelativistic and relativistic all-electron density functional calculations on the cationic sandwich complexes [Cp*M(η^6-C_6H_5Me)]$^{n+}$ (n = 2, M = Ir, Rh; n = 1, M = Ru) confirm that all three metals bind more tightly to Cp* than to toluene as gauged by the respective force constants ($k_1 > k_2$). A much larger relativistic enhancement of k_2 for M = Ir (279 vs 207 Nm^{-1}) could be responsible for the greater stability of Cp*Ir^{III} complexes in solution.

The analytical and synthetic perspectives of bioorganometallic chemistry have been highlighted in recent articles by Jaouen et al.[1] and Krämer[2]. Labeling of aromatic amino acid side-chains by η^6-coordinated transition metal half-sandwich fragments offers considerable potential in this respect. For instance, the group of Pearson[3] and Rich[4] has demonstrated that the diaryl coupling, required for the total synthesis of cyclic diphenyl ether peptides such as the protease inhibitor K-13, may be achieved under mild conditions by activation of protected *p*-Cl-phenylalanine through η^6-coordination of the CpRu^{II} fragment. We ourselves have recently employed both [(Cp*RuCl)$_2$(μ-Cl)$_2$] and [Cp*Ru(MeCN)$_3$]$^+$ for the first direct preparation of organometallic sandwich complexes of the free amino acids phenylalanine (L-HpheOH), tyrosine (L-HtyrOH) and tryptophan (L-HtrpOH)[5][6]. The feasibility of employing individual CpRu^{II}-coordinated amino acids for the construction of labeled peptides was demonstrated in the course of these activities by the synthesis of [Cp*Ru{η^6-cyclo-(phephe)}]$^+$ using the carbodiimide method[6].

Unfortunately, the applicability of the Cp*Ru^{II} fragment in the bioorganometallic field is restricted by the relative instability of its sandwich complexes in aqueous solution[5], a state of affairs that prompted us to investigate the suitability of alternative transition metal half-sandwich compounds. After recently reporting on η^6-CyRu^{II} complexes (Cy = *p*-cymene) of aromatic amino acids and peptides[7][8], we have now turned our attention to the compounds [Cp*IrL$_3$](CF_3SO_3)$_2$ [L = thf (**1a**), $(CH_3)_2CO$ (**1b**)] and [Cp*RhL$_3$](CF_3SO_3)$_2$ [L = thf (**2a**), $(CH_3)_2CO$ (**2b**), CH_3CN (**2c**)][9][10].

Results

In contrast to the tris(acetonitrile) half-sandwich complex [Cp*Ru(MeCN)$_3$](CF_3SO_3), which affords the entropically favoured sandwich compounds on treatment with free aromatic amino acids in thf[6], the analogous reaction of [CyRu(acetone)$_3$](CF_3SO_3)$_2$ leads[7][8] to formation of κ^2*N*,*O*-chelated products in CH_2Cl_2. Under such conditions, bis(η^6-arene)Ru^{II} sandwich compounds can only be prepared for fully protected amino acids such as *N*-acetyltyrosine ethyl ester (ActyrOEt). η^6-Coordination of the CyRu^{II} fragment by half-protected or free aromatic amino acids can, however, be achieved by carrying out the reaction in CF_3COOH. Protonation of the amino and/or carboxylato groups under such strongly acid conditions prevents their participation in the metal coordination sphere.

Similar considerations also apply to the Cp*Ir^{III} and Cp*Rh^{III} half-sandwich fragments. However, in these cases, the aromatic ring systems of *N*-protected amino acids such as *N*-acetyltyrosine (ActyrOH) can be successfully labeled in

  1434–1948/98/1212–1991 $ 17.50+.50/0

thf, as, for instance, in $[Cp^*Rh(ActyrOH)](CF_3SO_3)_2$ without competition from κ^1O-coordinated species. Sandwich complexes of *O*-protected or free amino acids are obtained in good yield (68−85%) by heating the reactants to 50°C for 24 h in CF_3COOH. ^{13}C-NMR spectra reveal a consistent pattern of upfield shifts of ca. 20−40 ppm for the signals of carbon atoms directly coordinated to the metal atom in comparison to those registered for the aromatic amino acids themselves. The formation of sandwich compounds is also confirmed by characteristic lowfield shifts for the ^{1}H-NMR signals of the Cp^*M^{III} (M = Ir, Rh) methyl protons. Furthermore, the typical chemical shift ranges of δ = 1.94−2.08, 2.25−2.28 and 2.40−2.44, in CD_3OD, associated with respectively η^6-coordinated tryptophan, tyrosine and phenyalanine derivatives, allow a straightforward assignment of the Cp^*Ir^{III} site in mixed oligopeptides. The marked kinetic instability of the analogous Cp^*Rh^{III} sandwich complexes in polar solvents prevents a general employment of this fragment in chemoselective organometallic labeling. However, our limited results indicate that a discrimination between η^6-coordinated tryptophan (δ = 1.96 in **11**) and tyrosine (δ = 2.09−2.20 in **6**−**8**) derivatives should once again be feasible.

η^5-Oxohexadienyl Coordination of Tyrosine Derivatives

Coordination to the Cp^*Ru^{II} and Cp^*M^{III} (M = Rh, Ir) fragments[10][11][12][13] stabilizes the ketonic form of phenol and its derivatives, leading to a marked enhancement in the acidity of the *p*-hydroxy substituent. Distortion towards an η^5-oxohexadienyl coordination mode in such sandwich complexes may be gauged from the shortness of the C−O bond distance and the degree of tilting between the plane of the *m*- and *p*-carbon atoms and the rest of the aromatic ring as expressed in the apposite dihedral angle θ. Relatively large θ values of 19° in $[Cp^*Ir(C_6H_3Me_2O)](BF_4)$[14], 14° in $[Cp^*Rh(C_6H_5O)](BF_4)\cdot H_2O$[13] and 13.2° in $[CyRu(HtyrOH)](CF_3SO_3)_2$[8] are accompanied by short C−O distances of 1.23, 1.25 and 1.274 Å, that are indicative of a pronounced degree of double-bond character. These structures differ markedly from that of $[Cp^*Ru(C_6H_5O)]\cdot 2$ PhOH[12] in which the phenol ring system is almost flat [θ = 4°, *d* (C−O) = 1.28 Å].

In $CyRu^{II}$ sandwich complexes, the *p*-hydroxy function of tyrosine derivatives is effectively fully deprotonated in aqueous solution. The concomitant increase in shielding for the aromatic ring protons causes their resonances to move upfield to values between δ = 5.6 and 6.6 in D_2O solution[8]. An analogous state of affairs is apparent for the Cp^*Ir^{III} complexes $[Cp^*Ir(ActyrOEt)](CF_3SO_3)_2$ (**3a**), $[Cp^*Ir(HtyrOMe)](CF_3SO_3)_2$ (**4**) and $[Cp^*Ir(HtyrOH)](CF_3SO_3)_2$ (**5**, HtyrOMe = tyrosine methyl ester) prepared in this work. The upfield shift is most pronounced for the *m*-protons adjacent to the tyrosine hydroxy function which are registered as separate doublets. Formation of the *N*-protonated zwitterions of HtyrOMe and HtyrOH further facilitates deprotonation of this aromatic substituent in **4** and **5** and leads of an additional upfield shift for the H atoms to δ = 5.83 and 5.86 in comparison to δ = 6.20 for **3a** in CD_3OD solution. This interpretation is confirmed by the remarkable ^{13}C-NMR chemical shifts of δ = 164.9 and 163.7 for the *p*-hydroxy-substituted tyrosine carbon atoms in **4** and **5**, values that are indicative of pronounced double-bond character for the associated C−O bonds. The analogous ^{13}C-NMR signal for **3a** at δ = 157.7 is registered only ca. 4 ppm downfield to that observed in free tyrosine derivatives. In contrast to the analogous Cp*Rh complexes **6**−**8**, the Cp*Ir sandwich complexes **3**−**5** of tyrosine derivatives are indefinitely stable in polar solvents such as water and methanol over a period of 14 days.

Scheme 1. Sandwich cations of $[Cp^*M(R'tyrOR)](CF_3SO_3)_2$ (**3**−**8**); **3a**: M = Ir, R = Et, R′ = Ac; **4**: M = Ir, R = Me, R′ = H; **5**: M = Ir, R = R′ = H; **6**: M = Rh; R = Et, R′ = Ac; **7**: R = H, R′ = Ac; **8**: M = Rh, R = Me, R′ = H

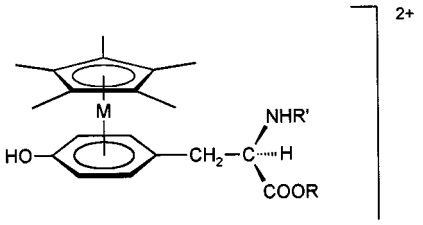

Attempts to obtain suitable crystals for X-ray-structural analysis unfortunately remained unsuccessful for **4** and **5** with their unprotected amino functions. However, colourless prisms of $[Cp^*Ir(ActyrOMe)](CF_3SO_3)_2$ (**3b**, ActyrOMe = *N*-acetyltyrosine methyl ester) could be grown by gas diffusion of diethyl ether into a methanol solution of $[Cp^*Ir(ActyrOH)](CF_3SO_3)_2$ prepared under similar conditions to **3a**. Solvent participation is apparent for the formation of η^6-coordinated ActyrOMe. The structure of the sandwich dication is depicted in Figure 1. Although the *p*-hydroxy oxygen atom O41 must be protonated for the fully protected tyrosine derivative ActyrOMe in the sandwich cation of **3b** [*d*(C34−O41) = 1.33(4) Å], the plane C33/C34/C35 is tilted by no less than θ = 12.9° from that of the remaining ring atoms C31−C33, C35 and C36. This pronounced departure from planarity may also be gauged from the Ir1−C34 distance of 2.36(4) Å, which is markedly longer than those to the remaining tyrosine ring atoms [2.22−2.30 Å]. The ^{1}H-NMR spectra of **3**−**5** in D_2O indicate that the tyrosine *p*-hydroxy function in Cp*Ir sandwich complexes is a moderately strong acid, a finding that is also reflected in the participation of O41 in relatively strong O41−H41···O21 hydrogen bonds of length 2.51 Å to the *N*-acetyl function of a symmetry-related complex cation. In view of the pronounced downfield shifts for the ^{13}C-NMR signal of C34 in **4** and **5**, for which the formation of *N*-protonated *O41*-deprotonated zwitterions is possible, it is reasonable to predict that the dihedral angle θ in these compounds will be even larger than in **3b** and perhaps close to that of 19° in $[Cp^*Ir(C_6H_3Me_2O)](BF_4)$[14].

Both Maitlis[10] and Jaouen[13] have commented on the instability of the sandwich complex $[Cp^*Rh(\eta^6\text{-phenol})]^{2+}$

Scheme 2. Stabilization of the ketonic form of the aromatic side chain of ActyrOEt in the Cp^*Rh^{III} complex **6**

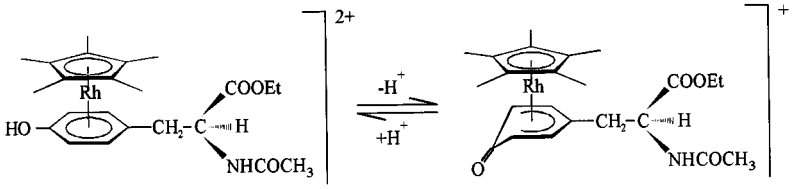

Figure 1. X-ray structure of the cation of $[Cp^*Ir(ActyrOMe)](CF_3SO_3)_2$ (**3b**)

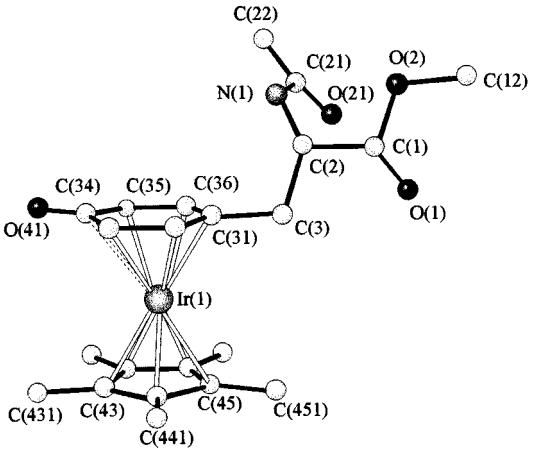

in polar solvents. Maitlis observed that $[Cp^*Rh)_2(phO)(phOH)](PF_6)_3$ is converted to 40% to $[(Cp^*Rh)_2(\mu\text{-}F_2PO_2)_3](PF_6)$ on standing for 48 h in acetone. Stabilization may be achieved by addition of base leading to formation of the η^5-oxocyclohexadienyl monocation $[Cp^*Rh(\eta^5\text{-}C_6H_5O)]^+$. Our time-dependent ^{1}H-NMR studies on $[Cp^*Rh(ActyrOEt)](CF_3SO_3)_2$ (**6a**) in D_2O solution, that are depicted in Figure 2, confirm a similar ca. 50% decay for the sandwich compound to $[Cp^*Rh(D_2O)_3]^{2+}$ and ActyrOEt within 24 hours at room temperature. A further ^{1}H-NMR spectrum taken after 5 days is similar to that of Figure 2c. It is interesting to note that Jaouen has postulated that the triflate counter anion $CF_3SO_3^-$ may stabilize the phenolic form of π-bonded arenes by participating in hydrogen bonds to the OH substituent of the aromatic ring system. For instance, whereas $[Cp^*Ir(\eta^6\text{-phenol})](BF_4)(CF_3SO_3)$ was very stable in aqueous solution, $[Cp^*Ir(\eta^6\text{-phenol})](BF_4)_2$ rapidly decays to a half-sandwich complex and could not be isolated. We have, therefore, performed comparative ^{1}H-NMR kinetic studies on $[Cp^*Rh(ActyrOEt)](PF_6)_2$ (**6b**) and $[Cp^*Rh(ActyrOEt)](BF_4)_2$ (**6c**) in D_2O solution. Suprisingly, whereas **6b** exhibits a decay rate similar to that of **6a**, as displayed in Figure 3 for **6c**, the sandwich cation $[Cp^*Rh(ActyrOEt)]^{2+}$ exhibits long-term stability in the presence of BF_4^- counter anions. Only ca. 20% formation of $[Cp^*RhL_3]^{2+}$ and ActyrOEt is apparent after 7 days. This finding suggests that a more subtle interplay of opposing factors may be responsible for the stabilizing effect of a particular anion.

Distortion towards the η^5-oxohexadienyl coordination mode in the Cp^*Rh^{III} sandwich complexes **6** and **7** leads the ^{1}H-NMR signals of the aromatic tyrosine protons to shift upfield to δ values between 5.8 and 6.6 in polar solvents (see Figures 2a and 3a). Figure 4 depicts the aromatic regions of the ^{1}H-NMR spectrum of $[Cp^*Rh(ActyrOEt)](CF_3SO_3)_2$ (**6a**) in (a) D_2O and (b) CD_3NO_2. In view of the instability of **6**–**8** in polar solvents, NMR data for these compounds are only reported for the latter solvent in the Experimental Section of this paper. It is interesting to note that the increase in shielding for the tyrosine *meta* protons of **6a** (δ = 5.82) in CD_3OD is similar to those of **4** and **5** (δ = 5.83 and 5.86) with their unprotected tyrosine amino functions. We were successful in growing suitable crystals of **6a** by gas diffusion of diethyl ether into a methanol solution and Figure 5 shows the X-ray structure of the sandwich cation in this compound. The dihedral angle θ of 5.09° is associated with a C34–O41 distance of 1.34(1) Å and is smaller than in the analogous Cp^*Ir^{III} complex **3b**. Distortion towards the η^5-oxohexadienyl coordination mode may also be gauged from the Rh1–C34 bond length of 2.339(8) Å, which is markedly longer than those to the remaining aromatic carbon atoms in the range 2.243(9)–2.259(7) Å. As in **3b**, relatively strong O–H···O hydrogen bonds [d(O41–H41···O21) = 2.51 Å] are present between the hydroxy and *N*-acetyl oxygen atoms of neighbouring dications. The triflate counter ions participate in weaker O···N1–H1 interactions of length 2.91 Å to the amide proton of N1.

Figure 2. Time-dependent ^{1}H-NMR spectra of $[Cp^*Rh(ActyrOEt)](CF_3SO_3)_2$ (**6a**) in D_2O at room temperature: (a) after 5 min, (b) after 1.5 h and (c) after 24 h

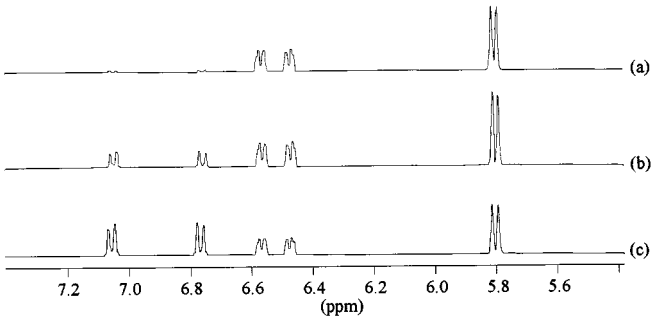

Compound **7** with ActyrOH as sandwich ligand was recrystallized from an acetone/hexane solution for X-ray analysis and displays a structure similar to that of **6a**. Tilting of the C33/C34/C35 plane leads to a Rh1–C34 distance of 2.337(11) Å and a dihedral angle θ of 2.97°. O41 exhibits a C34–O41 bond length of 1.31(1) Å and once again participates in intermolecular O–H···O hydrogen bonding to the *N*-acetyl O21 oxygen atom. It is interesting to note that whereas the metal–ring distances to the Cp* planes in **3b**,

Figure 3. Time-dependent ^{1}H-NMR spectra of [Cp*Rh(ActyrOEt)]$(BF_4)_2$ (**6c**) in D_2O at room temperature: (a) after 5 min, (b) after 48 h and (c) after 7 d

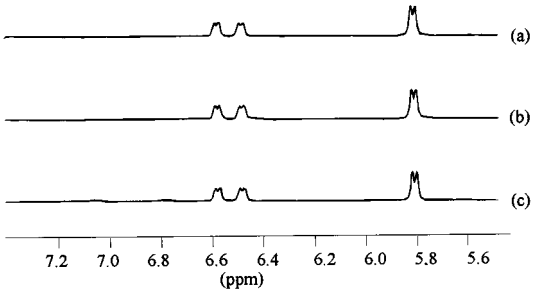

Figure 4. Aromatic regions of the ^{1}H-NMR spectra of [Cp*Rh(ActyrOEt)]$(CF_3SO_3)_2$ (**6a**) in (a) D_2O and (b) CD_3NO_2

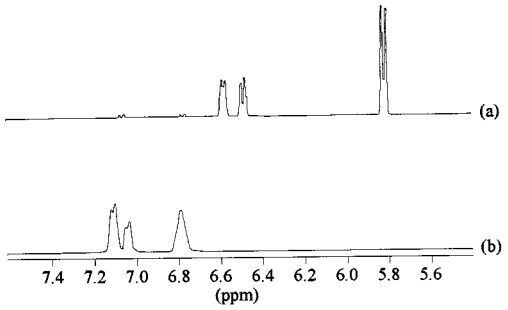

Figure 5. X-ray structure of the cation of [Cp*Rh(ActyrOEt)]$(CF_3SO_3)_2$ (**6a**)

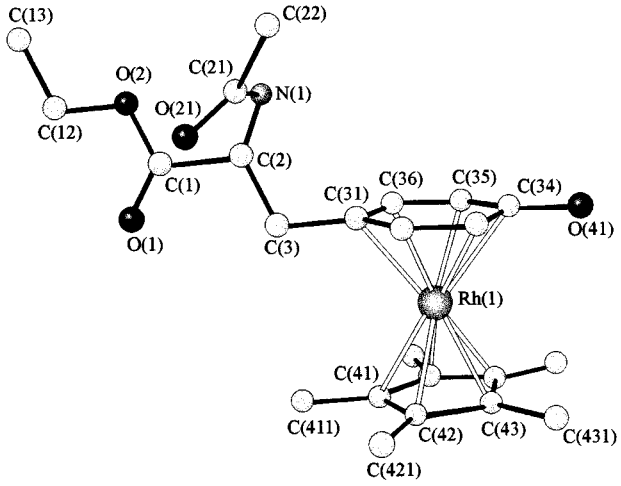

6a and **7** are all very similar [1.817, 1.807 and 1.796 Å], the opposite Ir-η^5-ActyrOMe distance in **3b** [1.738 Å] is markedly shorter than the analogous values for Rh^{III} in **6a** and **7** [1.763 and 1.771 Å].

[Cp*Rh(HtyrOMe)]$(CF_3SO_3)_2$ (**8**) decays immediately in polar solvents to the starting materials and ^{1}H-NMR spectra could, therefore, only be recorded in CD_3NO_2. This typical instability of Cp*Rh^{III} sandwich compounds of *N*-unprotected aromatic amino acids also prevents the isolation of the analogous π-bonded dication of tyrosine itself. Formation of an *N*-protected zwitterion allows effectively complete deprotonation of the tyrosine *p*-hydroxy function in **8** even in CD_3OD, as evidenced by the upfield shift of the *meta* proton doublets to δ = 5.54 and 5.58 in this solvent. The pronounced downfield shift of the ^{13}C-NMR signal for *C*OH from δ = 147.2 in **7** to 156.3 in **8** (CD_3NO_2 solutions) underscores this interpretation for the *N*-unprotected tyrosine derivative.

Facial Chirality in Tryptophan Complexes

η^6-Coordination of the aromatic indole system in tryptophan derivatives allows the formation of diastereomers owing to the possibility of facial chirality (Scheme 3). As we have already demonstrated for $CyRu^{II}$ sandwich compounds[8], opposite shifts are characteristic for ^{1}H-NMR signals of the protons of the π-bonded arene ring system. For instance, the signals of the inner protons H^5 and H^6 appear at higher field in [Cp*Rh(ActrpOMe)]$(CF_3SO_3)_2$ [**11a**; δ = 6.67 (m)], whereas a pronounced lowfield shift to δ = 7.75 (m) is observed for the signals of the outer protons H^4 and H^7. Assignment was achieved by use of HMQC-TOCSY spectra. Metal coordination of the neighbouring indole six-membered ring also leads to a marked change in the electron-density distribution in the condensed pyrrole ring as evidenced by pronounced shifts to lower field for both the H^2 [^{1}H NMR: δ = 8.28, 8.33 (2 s, 1 H)] and C^2 [^{13}C NMR: δ = 141.4] resonances of **11a** in CD_3NO_2 solution. Similar shifts were recorded for the analogous signals of the Cp*Ir^{III} sandwich compounds **9** and **10**, whose ^{1}H- and ^{13}C-NMR spectra were recorded in CD_3OD and D_2O solutions, respectively. The H^2 singulets for the α and β isomers are well resolved in **9**, **10** and **11a** and their integral values indicate that both diastereomers must be present in a ca. 1:1 ratio in all three compounds. After successful fractional crystallization, the H^2 resonance at higher field could be assigned to the diastereomer of [CyRu(ActrpOMe)]-$(CF_3SO_3)_2$ with β-facial chirality. It seems reasonable to assume that the same face of ActrpOMe is also preferred in [Cp*Rh(ActrpOMe)]$(PF_6)_2$ (**11a**) for which the H^2 signals [^{1}H NMR: δ = 8.27, 8.32 (2 s, 1 H)] are observed at the integral ratio of ca. 6:1 in CD_3NO_2. Whereas the Cp*Ir^{III} sandwich complexes **9** and **10** are stable over a period of 14 days in aqueous solution, both **11b** and the analogous compound [Cp*Rh(ActrpOMe)]$(CF_3SO_3)_2$ (**11a**) rapidly decay to ActrpOMe and appropriate tris(solvent) half-sandwich complex in water and methanol.

Stability of Cp*Ir^{III} and Cp*Rh^{III} Complexes in Solution

This relative instability of Cp*Rh^{III} sandwich complexes is also apparent for phenylalanine and its derivatives. As for the aromatic indole system of tryptophan, η^6-coordination can only be achieved with Cp*Rh^{III} when both the amino and carboxyl functions are protected. In accordance with similar observations for the analogous tyrosine and tryptophan complexes [Cp*Rh(AcpheOMe)]$(CF_3SO_3)_2$ (**14**) decays rapidly in polar solvents. ^{1}H-NMR signals for the aromatic protons of both this and the Cp*Ir^{III} sandwich compounds [Cp*Ir(AcpheOMe)]$(CF_3SO_3)_2$ (**12**) and [Cp*

Scheme 3. α and β isomers of [Cp*M(R′trpOR)]$(CF_3SO_3)_2$ (**9**−**11**); **9**: M = Ir, R = Me, R′ = Ac; **10**: M = Ir, R = R′ = H; **11**: M = Rh, R = Me, R′ = Ac

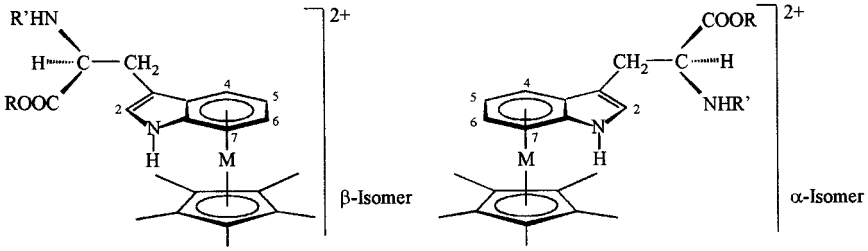

$Ir(H_2pheOMe)](CF_3SO_3)_3$ (**13**) lie in a close range (δ = 7.26−7.65) and are shifted marginally to lower field in comparison those of the free amino acid. The X-ray structure of the complex cation of **12** is depicted in Figure 6. Similar Ir−C distances [2.209−2.277 Å] are observed for all carbon atoms of the phenyl ring which itself is effectively planar.

Scheme 4. Sandwich cations of [Cp*M(R′pheOMe)]$(CF_3SO_3)_n$ (**12**−**14**); **12**: M = Ir, R′ = Ac, *n* = 2; **13**: M = Ir, R′ = H_2, *n* = 3; **14**: M = Rh, R′ = Ac, *n* = 2

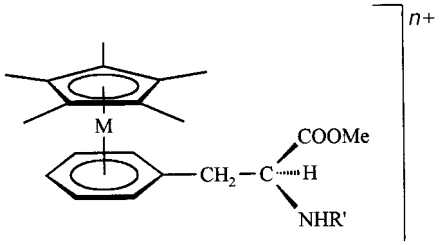

Figure 6. X-ray structure of the cation of [Cp*Ir(AcpheOMe)]$(CF_3SO_3)_2$ (**12**)

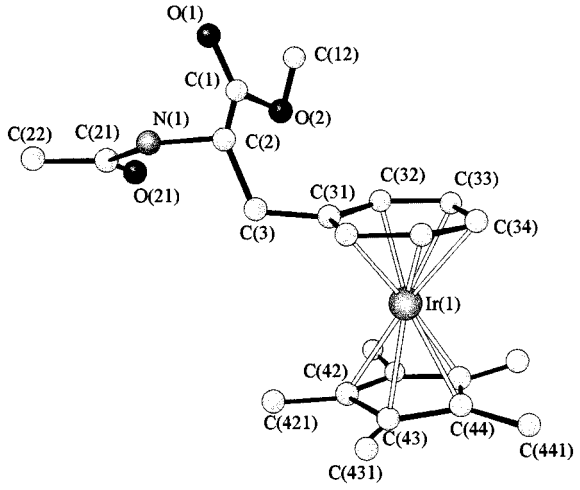

Although the greater stability of Cp^*Ir^{III} sandwich compounds in comparison to their rhodium analogues has been commented upon[15][16], attempts to fully understand this phenomenon still remain somewhat unsatisfactory. The introduction of π-arenes such as benzene or the cyclopentadienyl ion into hexaaqua cations $[M(H_2O)_6]^{2+}$ leads to a drastic increase in the lability of the three remaining water molecules, an effect that is more pronounced for anionic ligands[17]. This behaviour may be understood as a manifestation of the general principle that metal atoms usually tend to prefer either *hard* or *soft* ligands in their coordination spheres but not both at the same time[15]. Koelle et al. have demonstrated[17] that water exchange in half-sandwich triaqua complexes $[Cp^*M(H_2O)_3]^{2+}$ is faster by a factor of 6.3 for Rh^{III} in comparison to Ir^{III}.

Studies by Merbach[18] on the ligand-exchange reactions of $[Cp^*ML_3]^{2+}$ (L = CH_3CN, dmso) indicate that a dissociative mechanism must be involved. As previously reported by Maitlis[18], dmso was found to coordinate Rh^{III} through its oxygen, to Ir^{III} through its sulfur atom. Both this behaviour and the enhanced stability of Cp^*Ir^{III} sandwich compounds in polar solvents are in accordance with an increased preference of the heavier group-9 metal for *softer* ligands (e.g. π-arenes, κ*S*-dmso) in its coordination sphere. Of the members of the Co triad, Rh^{III} should be electronically best equipped to accommodate both *soft* and *hard* ligands in its coordination sphere, as is indeed suggested by the rapid decay of Cp^*Rh^{III} sandwich compounds to species $[Cp^*RhL_3]^{2+}$ in polar solvents (L = H_2O, CH_3OH).

Relativistic Effects

In structural organometallic chemistry, the consideration of relativistic effects[19] is essential to understand trends within a transition-metal triad, especially when going from the second to the third row. Classically speaking, electrons in heavy atoms move so fast that their velocity becomes comparable to the velocity of light. This leads to a contraction and stabilization of s- and p-orbitals but to an expansion and destabilization of d- and f-orbitals. The relativistic destabilization of the 5-d shell results in an increased softness of third-row transition metals.

The importance of relativistic effects can only indirectly be estimated from experiment (e.g. from unexpected trends in the periodic table) since nature is inherently relativistic. Quantum-mechanical calculations on the other hand can be performed either with or without taking care of relativity, and the difference between such computational results indicates the magnitude of relativistic effects. For transition-metal compounds, one generally finds a contraction and stabilization of metal−ligand bonds. These effects lead to similar molecular structures, but higher binding energies if isostructural complexes of homologous 4d and 5d metals are compared.

We have carried out nonrelativistic and relativistic all-electron density functional calculations on the $[Cp^*Rh(\eta^6\text{-}C_6H_5Me)]^{2+}$, $[Cp^*Ir(\eta^6\text{-}C_6H_5Me)]^{2+}$ and $[Cp^*Ru(\eta^6\text{-}C_6H_5Me)]^{+}$ cationic sandwich complexes. For details of the computational method, the reader is referred to ref.[20]. A full geometry optimization has been performed, and the force constants of the two coordinates describing the metal−ring distances have been evaluated. It is suggested that these force constants, which indicate how tightly the aromatic rings are bound to the metal atom, may serve as a measure for the *kinetic* stability of the complexes. Some results of these calculations have been collected in Table 1. The relativistic results are given, together with the results from the nonrelativistic calculations in parentheses. Both aromatic rings are essentially planar, and the coordinates d_1 and d_2 (Figure 7) are the distance between the metal atom and the planes of the Cp* and toluene aromatic ring, respectively. The force constants k_1 and k_2 are the second derivatives of the total energy with respect to the coordinates d_1 and d_2. For $[Cp^*Ir(\eta^6\text{-}C_6H_5Me)]^{2+}$, we can compare the calculated metal−ring distances (1.841 and 1.792 Å) to the X-ray result for $[Cp^*Ir(\eta^6\text{-AcpheOMe})](CF_3SO_3)_2$ (**12**; 1.811 and 1.744 Å) and find reasonable agreement. The nonrelativistic calculations give much larger values especially for the distance between iridium and the toluene ring (nonrelativistic: 1.925 Å, relativistic: 1.792 Å). As relativistic-effects scale with the square of the nuclear charge, the bond contractions are much smaller for the Rh (Z = 45) compounds than for Ir (Z = 77) complexes. Looking at the force constants, we find that both metals bind more tightly to Cp* than to toluene ($k_1 > k_2$). This is consistent with the experimental finding that in the first stages of the decay, the Cp^*Rh^{III} or Cp^*Ir^{III} units remain intact. For the kinetic stability of the complex, the value of k_2 appears to be most important. The calculations find 207 and 279 Nm^{-1}, respectively, for the Rh^{III} and Ir^{III} sandwich complexes, consistent with the much higher stability of the latter. This does not follow from the nonrelativistic data: it is the much larger relativistic enhancement of k_2 that makes the iridium complex so stable.

Figure 7. Definition of the distances d_1, d_2 and the force constants k_1, k_2 in sandwich cations of the type $[Cp^*M(\eta^6\text{-}C_6H_5Me)]^{n+}$ (n = 2, M = Ir, Rh; n = 1, M = Ru)

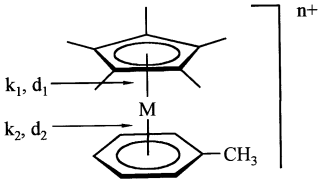

Similar calculations for $[Cp^*Ru(\eta^6\text{-}C_6H_5Me)]^{+}$ are also included in Table 1 and indicate as for the analogous Cp* Rh^{III} sandwich cation that relativistic effects are less marked for second-row transition metals. The distances presented for d_1 and d_2 [1.840 and 1.751 Å] may be compared with the average experimental values[6] of 1.816 and 1.704 Å in $[(Cp^*Ru)_2\{cyclo\text{-(phephe)}\}]^{2+}$. Despite the much shorter distance to the η^6-coordinated toluene ligand the force constants k_1 and k_2 are in accordance with tighter binding to Cp*, although the difference is less pronounced than in the Cp^*Ir^{III} and Cp^*Rh^{III} sandwich complexes.

Table 1. Metal−ring distances and force constants for $[Cp^*Rh(\eta^6\text{-}C_6H_5Me)]^{2+}$, $[Cp^*Ir(\eta^6\text{-}C_6H_5Me)]^{2+}$ and $[Cp^*Ru(\eta^6\text{-}C_6H_5Me)]^{+}$ from relativistic density functional calculations; nonrelativistic results are given in parentheses

Compound	d_1 [Å]	d_2 [Å]	k_1 [Nm^{-1}]	k_2 [Nm^{-1}]
$[Cp^*Rh(\eta^6\text{-}C_6H_5Me)]^{2+}$	1.840	1.830	358	207
	(1.862)	(1.876)	(334)	(182)
$[Cp^*Ir(\eta^6\text{-}C_6H_5Me)]^{2+}$	1.841	1.792	413	279
	(1.908)	(1.925)	(351)	(193)
$[Cp^*Ru(\eta^6\text{-}C_6H_5Me)]^{+}$	1.840	1.751	367	299
	(1.861)	(1.781)	(346)	(269)

Experimental Section

All manipulations and reactions were performed under argon in carefully dried solvents using standard Schlenk techniques. − FTIR[20]: Perkin-Elmer 1760; in KBr. − FAB MS: Fisons VG Autospec with 3-nitrobenzyl alcohol as the matrix. − ^1H and ^{13}C NMR: Bruker DRX 400; chemical shifts are reported as δ values relative to the signal of the deuterated solvent. − Elemental analyses were performed by Beller, Mikroanalytisches Labor, Göttingen. − The starting compounds $[(\eta^5\text{-}Cp^*)IrL_3](CF_3SO_3)_2$ [L = thf (**1a**), $(CH_3)_2CO$ (**1b**)] and $[(\eta^5\text{-}Cp^*)RhL_3](CF_3SO_3)_2$ [L = thf (**2a**), $(CH_3)_2CO$ (**2b**), CH_3CN (**2c**)] were prepared from respectively $[(\eta^5\text{-}Cp^*)IrCl_2]_2$ or $[(\eta^5\text{-}Cp^*)RhCl_2]_2$ by addition of an appropriate quantity of $Ag(CF_3SO_3)$ and filtration of the precipitated AgCl in the chosen solvent L[10]. Amino acids were purchased from Bachem (Heidelberg) and Calbiochem-Novabiochem (Bad Soden) and were used as received.

$[(\eta^5\text{-}Cp^*)Ir(ActyrOEt)](CF_3SO_3)_2$ (**3a**): N-acetyltyrosine ethyl ester (ActyrOEt, 37.2 mg, 0.15 mmol) was added to a solution of **1a** (122.6 mg, 0.15 mmol) in 12 mL of thf and the reaction mixture heated at reflux for 18 h. The resulting solid was stirred for 24 h with diethyl ether and dried in vacuo after centrifugation to afford **3**. Yield 112 mg (86%). − $C_{25}H_{32}F_6IrNO_{10}S_2$ (876.5): calcd. C 34.3, H 3.7, N 1.6; found C 34.6, H 3.8, N 2.0. − FAB MS; *m/z* (%): 727 (1) $[M - CF_3SO_3]^+$, 578 (100) $[M - 2\ CF_3SO_3]^+$, 445 (3) $[M - 2\ CF_3SO_3 - NHAc - CO_2Et]^+$. − ^1H NMR (CD_3OD): δ = 1.32 (t, 3 H, C*H*$_3$ OEt), 2.04 (s, 3 H, C*H*$_3$ Ac), 2.28 (s, 15 H, C*H*$_3$ Cp*), 2.83/3.03 (2 dd, 2 H, β-C*H*$_2$), 4.27 (q, 2 H, C*H*$_2$ OEt), 4.79 (dd, 1 H, α-C*H*), 6.20 (2 d, 2 H, H_{meta} tyr), 6.70/6.78 (2 d, 2 H, H_{ortho} tyr). − ^{13}C NMR (CD_3OD): δ = 9.9 (*C*H$_3$ Cp*), 14.7 (*C*H$_3$ OEt), 22.7 (*C*H$_3$ Ac), 35.0 (β-*C*), 54.1 (α-*C*), 63.5 (*C*H$_2$ OEt), 84.1 (C_{meta} tyr), 97.9 (C_{ortho} tyr), 102.0 (*C*CH$_3$ Cp*), 103.2 (*C* tyr), 157.7 (*C*OH tyr), 171.4 (*C*OO), 173.8 (NH*C*O). − IR: $\tilde{\nu}$ = 3273 s (NH), 1743 s (CO), 1582, 1531 m (NH) cm^{-1}.

$[(\eta^5\text{-}Cp^*)Ir(HtyrOMe)](CF_3SO_3)_2$ (**4**): Tyrosine methyl ester (HtyrOMe, 38 mg, 0.2 mmol) was stirred with **1b** (160 mg, 0.2 mmol) for 24 h in 12 mL of CF_3COOH at 50°C and the solution reduced in volume to 3 mL. After precipitation with diethyl ether, the resulting solid was dried in vacuo to afford **4**. Yield 139.5 mg (85%). − $C_{22}H_{28}F_6IrNO_9S_2$ (820.8): calcd. C 32.2, H 3.4, N 1.7; found C 32.1, H 3.6, N 1.5. − FAB MS; *m/z* (%): 522 (100) $[M - 2\ CF_3SO_3]^+$. − ^1H NMR (CD_3OD): δ = 2.25 (s, 15 H, C*H*$_3$ Cp*), 3.04 (2 dd, 2 H, β-C*H*$_2$), 3.91 (s, 3 H, COC*H*$_3$), 4.55 (dd, 1 H, α-C*H*), 5.83 (2 d, 2 H, H_{meta} tyr), 6.51, 6.57 (2 d, 2 H, H_{ortho} tyr). −

^{13}C NMR (CD_3OD): δ = 10.8 (CH_3 Cp*), 34.6 (β-*C*), 55.0 (α-*C*), 55.5 (CH_3OMe), 84.0, 84.2 (C_{meta} tyr), 97.2, 98.7 (C_{ortho} tyr), 99.3 (CCH_3 Cp*), 103.1 (*C* tyr), 164.9 (*C*OH tyr), 170.3 (*C*OO). − IR: $\tilde{\nu}$ = 3284 s (NH), 1746 s (CO), 1573 m (NH) cm^{-1}.

[(η5-Cp)Ir(HtyrOH)](CF3SO3)2* (**5**): The preparation was performed with tyrosine (27.9 mg, 0.15 mmol) and **1a** (128 mg, 0.15 mmol) in CF_3COOH in an analogous manner to **4**. Yield 82.2 mg (68%). − $C_{21}H_{26}F_6IrNO_{10}S_2$ (806.2): calcd. C 31.3, H 3.2, N 1.7; found C 31.1, H 3.5 N 1.7. − FAB MS; *m/z* (%): 658 (1) [M − CF_3SO_3]$^+$, 508 (100) [M − 2 CF_3SO_3]$^+$, 462 (6) [M − 2 CF_3SO_3 − CO_2H]$^+$. − ^{1}H NMR (CD_3OD): δ = 2.26 (s, 15 H, CH_3 Cp*), 3.03 (m, 2 H, β-CH_2), 4.49 (dd, 1 H, α-C*H*), 5.86 (2 d, 2 H, H_{meta} tyr), 6.59, 6.63 (2 d, 2 H, H_{ortho} tyr). − ^{13}C NMR (CD_3OD): δ = 9.9 (CH_3 Cp*), 33.7 (β-*C*), 54.1 (α-*C*), 83.1 (C_{meta} tyr), 97.4 (C_{ortho} tyr), 98.5 (*C* tyr), 102.2 (CCH_3 Cp*), 163.7 (*C*OH tyr), 170.1 (*C*OO). − IR: $\tilde{\nu}$ = 3178 s (NH), 1742 s (CO), 1559 m (NH) cm^{-1}.

[(η5-Cp)Rh(ActyrOEt)](CF3SO3)2* (**6a**): ActyrOEt (75.4 mg, 0.3 mmol) and **2b** (213.2 mg, 0.3 mmol) were stirred for 2 d in 15 mL of thf and the resulting solid removed by centrifugation. After washing with diethyl ether, the product was dried to afford **6.** Yield 198.5 mg (84%). Recrystallization by gas diffusion of diethyl ether into a methanol solution provided suitable crystals for X-ray analysis. − $C_{25}H_{32}F_6NO_{10}RhS_2$ (787.6): calcd. C 38.1, H 4.1, N 1.8; found C 37.6, H 4.0, N 1.8. − FAB MS; *m/z* (%): 637 (1) [M − CF_3SO_3]$^+$, 488 (100) [M − 2 CF_3SO_3]$^+$, 237 (11) [M − 2 CF_3SO_3 − ActyrOEt]$^+$. − ^{1}H NMR (CD_3NO_2): δ = 1.21 (t, 3 H, CH_3 OEt), 1.93 (s, 3 H, CH_3 Ac), 2.19 (s, 15 H, CH_3 Cp*), 2.97, 3.16 (2 dd, 2 H, β-CH_2), 4.17 (q, 2 H, CH_2 OEt), 4.79 (dd, 1 H, α-C*H*), 6.79 (2 d, 2 H, H_{meta} tyr), 7.05, 7.18 (2 d, 2 H, H_{ortho} tyr). − ^{13}C NMR (CD_3NO_2): δ = 8.9 (CH_3 Cp*), 12.8 (CH_3 OEt), 21.1 (CH_3 Ac), 33.6 (β-*C*), 52.3 (α-*C*), 62.1 (CH_2 OEt), 93.8 (C_{meta} tyr), 106.3, 106.5 (C_{ortho} tyr), 110.9 (CCH_3 Cp*), 112 (*C* tyr), 147.2 (*C*OH tyr), 169.4 (*C*OO), 171.5 (NH*C*O). − IR: $\tilde{\nu}$ = 3274 s (NH), 1742 s (CO), 1539 m (NH) cm^{-1}.

[(η5-Cp)Rh(ActyrOH)](CF3SO3)2* (**7**): The preparation was performed with *N*-acetyltyrosine (ActyrOH, 66.7 mg, 0.3 mmol) and **2c** (198.1 mg 0.3 mmol) in a manner similar to **6** with the exception that the thf was refluxed for 16 h. Yield 177.7 mg (78%). Recrystallization by covering an acetone solution with hexane provided suitable crystals for X-ray analysis. − $C_{23}H_{28}F_6NO_{10}RhS_2$ (759.5): calcd. C 36.4, H 3.7, N 1.8; found C 36.0, H 3.7, N 1.6. − FAB MS; *m/z* (%): 609 (1) [M − CF_3SO_3]$^+$, 460 (100) [M − 2 CF_3SO_3]$^+$, 205 (11) [M − 2 CF_3SO_3 − ActyrOH]$^+$. − ^{1}H NMR (CD_3NO_2): δ = 1.97 (s, 3 H, CH_3 Ac), 2.20 (s, 15 H, CH_3 Cp*), 2.95, 3.20 (2 dd, 2 H, β-CH_2), 4.77 (dd, 1 H, α-C*H*), 6.76, 6.80 (2 d, 2 H, H_{meta} tyr), 6.90, 7.04 (2 d, 2 H, H_{ortho} tyr), 7.09 (s, 1 H, N*H*CO). − ^{13}C NMR (CD_3NO_2): δ = 8.9 (CH_3 Cp*), 21.1 (CH_3 Ac), 33.6 (β-*C*), 52.2 (α-*C*), 93.8 (C_{meta} tyr), 106.2, 106.6 (C_{ortho} tyr), 110.9 (CCH_3 Cp*), 111.6 (*C* tyr), 147.2 (*C*OH tyr), 170.1 (*C*OO), 171.6 (NH*C*O). − IR: $\tilde{\nu}$ = 3284 s (NH), 1749 s (CO), 1573 m (NH) cm^{-1}.

[(η5-Cp)Rh(HtyrOMe)](CF3SO3)2* (**8**): The preparation was performed with HtyrOMe (57 mg, 0.3 mmol) and **2b** (213.2 mg, 0.3 mmol) in a manner similar to **4** and **5**. Yield 177.7 mg (81%). − $C_{22}H_{28}F_6NO_9RhS_2$ (731.4): calcd. C 36.1, H 3.9, N 1.9; found C 36.0, H 3.7, N 1.8. − FAB MS; *m/z* (%): 582 (4) [M − CF_3SO_3]$^+$, 432 (100) [M − 2 CF_3SO_3]$^+$, 237 (23) [M − 2 CF_3SO_3 − HtyrOMe]$^+$. − ^{1}H NMR (CD_3NO_2): δ = 2.09 (s, 15 H, CH_3 Cp*), 3.22, 3.24 (2 dd, 2 H, β-CH_2), 3.83 (s, 3 H, COCH_3), 4.55 (dd, 1 H, α-C*H*), 5.54, 5.58 (2 d, 2 H, H_{meta} tyr), 6.48, 6.82 (2 d, 2 H, H_{ortho} tyr). − ^{13}C NMR (CD_3NO_2): δ = 8.7 (CH_3 Cp*), 34.5 (β-*C*), 53.3 (α-*C*), 55.5 (CH_3 OMe), 93.2, 94.4 (C_{meta} tyr), 105.7, 106.4 (C_{ortho} tyr), 109.0 (CCH_3 Cp*), 115.7 (*C* tyr), 156.3 (*C*OH tyr), 167.2 (*C*OO). − IR: $\tilde{\nu}$ = 1752 s (CO), 1590, 1522 m (NH) cm^{-1}.

[(η5-Cp)Ir(ActrpOMe)](CF3SO3)2* (**9**): N-Acetyltryptophan methyl ester (ActrpOMe, 40.4 mg, 0.16 mmol) and **1a** (128.7 mg, 0.16 mmol) were stirred in 10 ml of thf for 24 h at room temperature or heated at 45°C for 2 h. The resulting solid was then stirred for 24 h with diethyl ether and dried in vacuo to afford **9**. Yield 102 mg (72%). − $C_{25}H_{30}F_6IrN_2O_9S_2$ (885.5): calcd. C 35.3, H 3.4, N 3.1; found C 34.7, H 3.4, N 3.3. − FAB MS; *m/z* (%): 738 (53) [M − CF_3SO_3]$^+$, 588 (62) [M − 2 CF_3SO_3]$^+$, 527 (3) [M − 2 CF_3SO_3 − $COOCH_3$]$^+$. − ^{1}H NMR (CD_3OD): δ = 1.97, 2.02 (2 s, 3 H, CH_3 Ac), 2.08 (s, 15 H, CH_3 Cp*), 3.28, 3.41 (2 dd, 2 H, β-CH_2), 3.76, 3.82 (2 s, 3 H, CH_3 OMe), 4.87 (dd, 1 H, α-C*H*), 7.07 (m, 2 H, H_{ind}), 7.87 (dd, 1 H, H_{ind}), 8.01 (dd, 1 H, H_{ind}), 8.37, 8.42 (2 s, H_{ind}). − ^{13}C NMR (CD_3OD): δ = 9.4 (CH_3 Cp*), 22.8 (CH_3 Ac), 27.4 (β-*C*), 53.7 (α-*C*), 54.1 (*C*OMe), 84.7, 89.8, 91.3, 92.2 (C_{ind}), 103.3 (CCH_3 Cp*), 106.9, 116.2, 120.2, 143.5 (C_{ind}), 172.7 (NH*C*O), 173.8 (*C*OO). − IR: $\tilde{\nu}$ = 3323 s (NH), 1742 s, 1667 s (CO), 1541 m (NH) cm^{-1}.

[(η5-Cp)Ir(HtrpOH)](CF3SO3)2* (**10**): HtrpOH (39.8 mg, 0.195 mmol) was heated with **1a** (168.4 mg, 0.2 mmol) at 65°C in 12 ml of CF_3COOH for 48 h and the solution reduced in volume to 3 ml. After precipitation with diethyl ether the resulting solid was dried in vacuo to afford **10**. Yield 111.6 mg (69%). − $C_{23}H_{27}F_6IrN_2O_8S_2$ (829.8): calcd. C 33.3, H 3.3, N 3.4; found C 33.4, H 3.8, N 3.4. − FAB MS; *m/z* (%): 681 (3) [M − CF_3SO_3]$^+$, 531 (100) [M − 2 CF_3SO_3]$^+$. − ^{1}H NMR (D_2O): δ = 1.94 (s, 15 H, CH_3 Cp*), 3.43 (2 dd, 2 H, β-CH_2), 4.13, 4.22 (2 m, 1 H, α-C*H*), 6.95 (m, 2 H, H_{ind}), 7.74, 7.78, 7.86 (m, 2 H, H_{ind}), 8.36, 8.40 (2 s, 1 H, H_{ind}). − ^{13}C NMR (D_2O): δ = 8.3 (CH_3 Cp*), 26.0 (β-*C*), 52.2 (α-*C*), 88.1, 96.6, 97.0, 97.6 (C_{ind}), 101.9 (CCH_3 Cp*), 104.9, 114.2, 118.2, 141.4 (C_{ind}), 170.4 (*C*OO). − IR: $\tilde{\nu}$ = 1646 s (CO), 1518 m (NH) cm^{-1}.

[(η5-Cp)Rh(ActrpOMe)](CF3SO3)2* (**11a**): ActrpOMe (51.1 mg, 0.2 mmol) and **2b** (142.1 mg, 0.2 mmol) were stirred in 10 ml of thf for 48 h at room temperature. The resulting solid was subsequently stirred for 24 h with diethyl ether and dried in vacuo to give **11a**. Yield 108.3 mg (68%). − $C_{26}H_{31}F_6IrN_2O_9S_2$ (796.6): calcd. C 39.2, H 3.9, N 3.5; found C 39.0, H 3.7, N 3.4. − FAB MS; *m/z* (%): 498 (100) [M − 2 CF_3SO_3]$^+$, 237 (16) [M − 2 CF_3SO_3 − ActrpOMe]$^+$. − ^{1}H NMR (CD_3NO_2): δ = 1.84, 1.90 (2 s, 3 H, CH_3 Ac), 1.96 (s, 15 H, CH_3 Cp*), 3.30 (2 dd, 2 H, β-CH_2), 3.64, 3.72 (2 s, 3 H, CH_3 OMe), 4.76 (m, 1 H, α-C*H*), 6.67 (m, 2 H, H_{ind}), 7.75 (m, 2 H, H_{ind}), 8.28, 8.33 (2 s, 1 H, H_{ind}). − ^{13}C NMR (CD_3NO_2): δ = 8.3 (CH_3 Cp*), 21.2 (CH_3 Ac), 26.0 (β-*C*), 51.9 (CH_3 OMe), 52.2 (α-*C*), 88.1, 96.6, 97.0, 97.6 (C_{ind}), 108.7 (CCH_3 Cp*), 108.7, 111.4, 112.8, 141.4 (C_{ind}), 170.0, 170.4 (NH*C*O, *C*OO). − IR: $\tilde{\nu}$ = 3328 s (NH), 1741, 1657 s (CO), 1546 m (NH) cm^{-1}.

[(η5-Cp)Ir(AcpheOMe)](CF3SO3)2* (**12**): N-acetylphenylalanine methyl ester (AcpheOMe, 29.5 mg, 0.13 mmol) was added to a solution of **1a** (110.7 mg, 0.13 mmol) in 12 ml of thf and the suspension refluxed for 18 h. After removal of the solvent the resulting precipitate was stirred for 24 h with diethyl ether and dried in vacuo to afford **12**. Yield 84.7 mg (77%). Recrystallization by gas diffusion of diethyl ether into a methanol solution provided suitable crystals for X-ray analysis. − $C_{23}H_{30}F_6IrNO_9S_2$ (846.5): calcd. C 32.6, H 3.6, N 1.7; found C 33.9, H 3.6, N 1.5. − FAB MS; *m/z* (%): 548 (58) [M − 2 CF_3SO_3]$^+$, 4.89 (4) [M − 2 CF_3SO_3 − $COOCH_3$]$^+$. − ^{1}H NMR (CD_3OD): δ = 2.02 (2 s, 3 H, CH_3 Ac), 2.43 (s, 15 H, CH_3 Cp*), 3.09, 3.28 (2 dd, 2 H, β-CH_2), 3.81 (2 s, 3 H, CH_3 OMe), 4.88 (dd, 1 H, α-C*H*), 7.48 (m, 4 H, phe), 7.57 (t, 1 H_{para}, phe). − ^{13}C NMR (CD_3OD): δ = 10.4 (CH_3 Cp*), 22.7

(CH_3 Ac), 35.7 (β-*C*), 53.8 (α-*C*, CH_3 OMe), 99.6, 99.7 (*C* phe), 107.8 (CCH_3 Cp*), 115.4 (*C* phe), 171.6 (NH*C*O), 173.8 (*C*OO). IR: $\tilde{\nu}$ = 3386 s (NH), 1745 s, 1667 s (CO), 1533 m (NH) cm^{-1}.

[(η⁵-Cp)Ir(H₂pheOMe)](CF₃SO₃)₃* (**13**): HpheOMe·HCl (43.1 mg, 0.2 mmol) was dissolved in 10 mL of methanol and $AgCF_3SO_3$ (0.2 mmol, 51.4 mg) added to the solution. The precipated AgCl was removed by filtration and the solution dried in vacuo. The resulting solid was stirred with **1b** (160.0 mg, 0.2 mmol) in 12 mL of CF_3COOH for 24 h. After reduction of the solvent volume to 3 mL, addition of diethyl ether led to precipitation of **13** which was dried in vacuo. Yield 145.1 mg (76%). − $C_{23}H_{29}F_9IrNO_{11}S_3$ (954.9): calcd. C 28.9, H 3.1, N 1.5; found C 28.5, H 3.3, N 1.4. − FAB MS; *m/z* (%): 806 (20) $[M]^+$, 656.2 (16) $[M - CF_3SO_3]^+$, 506 (100) $[M - 2\ CF_3SO_3]^+$, 419 (27) $[Cp^*IrC_6H_5CH_2]^+$. − ^{1}H NMR (CD_3OD): δ = 2.44 (s, 15 H, CH_3 Cp*), 3.31 (2 dd, 2 H, β-CH_2), 3.89 (2 s, 3 H, CH_3 OMe), 4.62 (m, 1 H, α-C*H*), 7.65 (m, phe). − ^{13}C NMR (CD_3OD): δ = 10.4 (CH_3 Cp*), 33.7 (β-*C*), 53.5 (CH_3 OMe), 54.7 (α-*C*), 99.71, 100.1, 100.1, 100.3, 101.0 (*C* phe), 108.2 (CCH_3 Cp*), 112.7 (*C* phe), 168.9 (*C*OO). − IR: $\tilde{\nu}$ = 1756 s (CO), 1630, 1501 m (NH) cm^{-1}.

[(η⁵-Cp)Rh(AcpheOMe)](CF₃SO₃)₂* (**14**): AcpheOMe (51.1 mg, 0.2 mmol) was refluxed with **2b** (150.5 mg, 0.2 mmol) in 15 mL of thf for 20 h and the solution reduced in volume to 3 mL. After precipitation with *n*-hexane, the resulting solid was washed with diethyl ether and dried in vacuo to afford **14**. Yield 109.1 mg (72%). − $C_{24}H_{30}F_6NO_9RhS_2$ (757.5): calcd. C 38.1, H 4.0, N 1.9; found C 37.4, H 3.8, N 1.4. − FAB MS; *m/z* (%): 608 (3) $[M - CF_3SO_3]^+$, 459 (60) $[M - 2\ CF_3SO_3]^+$, 237 (15) $[M - 2\ CF_3SO_3 - AcpheOMe]^+$. − ^{1}H NMR ($CD_3NO_2$): δ = 1.42 (2 s, 3 H, C$H_3$ Ac), 2.11 (s, 15 H, CH_3 Cp*), 3.23 (2 dd, 2 H, β-CH_2), 3.61 (2 s, 3 H, CH_3 OMe), 4.12 (m, 1 H, α-C*H*), 7.26 (m, 5 H, phe). − ^{13}C NMR (CD_3NO_2): δ = 9.7 (CH_3 Cp*), 14.11 (CH_3 Ac), 37.5 (β-*C*), 52.9 (α-*C*), 65.1 (CH_3 OMe), 106.3, 107.1, 107.3, 107.6, 107.9 (*C* phe), 113.1, 113.2 (CCH_3 Cp*, *C* phe), 176.5 (NH*C*O), 177.5 (*C*OO). − IR: $\tilde{\nu}$ = 1668, 1744 (CO), 1541 (NH) cm^{-1}.

X-ray-Structural Analyses: Siemens P4 diffractometer, graphite-monochromated Mo-K_α radiation (λ = 0.71073 Å). Empirical absorption correction (DIFABS)[22] were applied to the reflection intensities for **6** and **12**. Semi-empirical absorption corrections were applied to the intensity data for **3b** and **7** by use of ψ scans. The structures were solved by direct methods or Patterson syntheses and refined by full-matrix least squares against F^2 using SHELXL-93[23]. Hydrogen atoms were included at calculated positions with isotropic temperature factors[24].

[(η⁵-Cp)Ir(ActyrOMe)](CF₃SO₃)₂* (**3b**): $C_{24}H_{30}F_6IrNO_{10}S_2$, M = 862.8, T = 295 K, orthorhombic, space group $P2_12_12_1$ (no. 19), a = 9.174(2), b = 13.133(3), c = 27.022(5) Å, V = 3255.7(12) Å^3, Z = 4, $D_{calcd.}$ = 1.760 g·cm^{-3}, μ = 4.31 mm^{-1}. Crystal size: 0.43 × 0.21 × 0.16 mm; ω scan; scan range: 4° ≤ 2 θ ≤ 45° (0 ≤ h ≤ 9, 0 ≤ k ≤ 14, 0 ≤ l ≤ 29), 2382 symmetry-independent reflections; max./min. transmission: 0.492/0.212; 143 parameters refined; R = 0.077 [$I > 2\ \sigma(I)$], wR_2 = 0.212 (all data), Δρ max./min. = 1.11/−1.56 e Å^{-3}. The Cp* ligand was refined as a rigid group.

[(η⁵-Cp)Rh(ActyrOEt)](CF₃SO₃)₂* (**6a**): $C_{25}H_{32}F_6NO_{10}RhS_2$, M = 787.6, T = 215 K, monoclinic, space group $P2_1$ (no. 4), a = 9.447(3), b = 12.835(2), c = 13.601(2) Å, β = 99.12(2)°, V = 1628.3(7) Å^3, Z = 2, $D_{calcd.}$ = 1.606 g·cm^{-3}, μ = 0.74 mm^{-1}. Crystal size: 0.79 × 0.69 × 0.31 mm; ω scan; scan range: 4° ≤ 2 θ ≤ 55° (−11 ≤ h ≤ 11, −3 ≤ k ≤ 16, −17 ≤ l ≤ 17), 4100 symmetry-independent reflections; 397 parameters refined; R = 0.056 [$I > 2\ \sigma(I)$], wR_2 = 0.158 (all data), Δρ max./min. = 1.04/−1.12 eÅ^{-3}.

[(η⁵-Cp)Rh(ActyrOH)](CF₃SO₃)₂* (**7**): $C_{23}H_{28}F_6NO_{10}RhS_2$, M = 759.5, T = 193 K, monoclinic, space group $P2_1$ (no. 4), a = 9.445(4), b = 12.558(4), c = 12.627(4) Å, β = 98.12(2)°, V = 1482.7(9) Å^3, Z = 2, $D_{calcd.}$ = 1.701 g·cm^{-3}, μ = 0.80 mm^{-1}. Crystal size: 0.76 × 0.32 × 0.22 mm; ω scan; scan range: 4° ≤ 2 θ ≤ 60° (−10 ≤ h ≤ 10, −3 ≤ k ≤ 14, −15 ≤ l ≤ 14), 4082 symmetry-independent reflections; parameters refined; R = 0.070 [$I > 2\ \sigma(I)$], wR_2 = 0.187 (all data), Δρ max./min. = 1.43/−1.61 eÅ^{-3}.

[(η⁵-Cp)Ir(AcpheOMe)](CF₃SO₃)₂* (**12**): $C_{24}H_{30}F_6IrNO_9S_2$, M = 846.8, T = 215 K, monoclinic, space group $P2_1$ (no. 4), a = 12.758(3), b = 9.051(3), c = 13.403(3) Å, β = 102.00(2)°, V = 1513.8(7) Å^3, Z = 2, $D_{calcd.}$ = 1.858 g·cm^{-3}, μ = 4.635 mm^{-1}. Crystal size: 0.47 × 0.23 × 0.18 mm; θ−2 θ scan; scan range: 4° ≤ 2 θ ≤ 50° (0 ≤ h ≤ 15, 0 ≤ k ≤ 10, −15 ≤ l ≤ 15), 2846 symmetry-independent reflections; 395 parameters refined; R = 0.049 [$I > 2\ \sigma(I)$], wR_2 = 0.141 (all data), Δρ max./min. = 3.72/−2.93 eÅ^{-3}. The Cp* ligand was refined as a rigid group.

[1] G. Jaouen, A. Vessières, I. S. Butler, *Acc. Chem. Res.* **1993**, *26*, 361−369.
[2] R. Krämer, *Angew. Chem.* **1996**, *108*, 1287−1289; *Angew. Chem. Int. Ed. Engl.* **1996**, *35*, 1197−1199.
[3] A. J. Pearson, K. Lee, *J. Org. Chem.* **1994**, *59*, 2304−2313.
[4] J. W. Janetka, D. H. Rich, *J. Am. Chem. Soc.* **1995**, *117*, 10585−10586.
[5] W. S. Sheldrick, A. J. Gleichmann, *J. Organomet. Chem.* **1994**, *470*, 183−187; A. J. Gleichmann, Dissertation, Ruhr-Universität Bochum, **1994**.
[6] A. J. Gleichmann, J. M. Wolff, W. S. Sheldrick, *J. Chem. Soc., Dalton Trans.* **1995**, 1549−1554; J. M. Wolff, A. J. Gleichmann, C. Schmidt, W. S. Sheldrick, *J. Inorg. Biochem.* **1995**, *59*, 219−219.
[7] J. M. Wolff, W. S. Sheldrick, *J. Organomet. Chem.* **1997**, *531*, 141−149.
[8] J. M. Wolff, W. S. Sheldrick, *Chem. Ber.* **1997**, *130*, 981−988.
[9] C. White, P. M. Maitlis, *J. Chem. Soc. A* **1971**, 3322−3326; V. Part, J. W. Kang, P. M. Maitlis, *J. Organomet. Chem.* **1971**, *30*, 127−133.
[10] C. White, S. J. Thompson, P. M. Maitlis, *J. Organomet. Chem.* **1977**, *127*, 415−421; C. White, S. J. Thompson, P. M. Maitlis, *J. Chem. Soc., Dalton Trans.* **1977**, 1654−1661.
[11] B. Chaudret, X. He, Y. Huang, *J. Chem. Soc., Chem. Commun.* **1989**, 1844−1846.
[12] U. Koelle, M. H. Wang, G. Raabe, *Organometallics* **1991**, *10*, 2573−2577.
[13] J. Le Bras, H. El Amouri, Y. Besace, J. Vaissermann, G. Jaouen, *Bull. Soc. Chim. Fr.* **1995**, *132*, 1073−1082.
[14] J. Le Bras, H. El Amouri, J. Vaissermann, *Organometallics* **1996**, *26*, 5706−5712.
[15] U. Koelle, *Coord. Chem. Rev.* **1994**, *135*, 623−650.
[16] P. M. Maitlis, *Acc. Chem. Res.* **1978**, *11*, 301−307.
[17] L. Dadci, H. Elias, U. Frey, A. Hörnig, U. Koelle, A. E. Merbach, H. Paulus, J. S. Schneider, *Inorg. Chem.* **1995**, *34*, 306−315.
[18] A. Cusanelli, L. Nicula-Dadci, U. Frey, A. E. Merbach, *Inorg. Chem.* **1997**, *36*, 2211−2217.
[19] P. Pyykkö, *Chem. Rev.* **1988**, *88*, 563−594.
[20] C. van Wüllen, *J. Comput. Chem.* **1997**, *18*, 1985−1992.
[21] C. S. Schmidt, Dissertation, Ruhr-Universität Bochum, **1998**.
[22] N. Walker, D. Stuart, *Acta Crystallogr., Sect. A* **1983**, *39*, 158−166.
[23] G. M. Sheldrick, *SHELXL-93, A Program for Structure Refinement*, Göttingen, **1993**.
[24] Crystallographic data (excluding structure factors) for the structures reported in this paper have been deposited with the Cambridge Crystallographic Data Centre. Copies of the data (deposition numbers CCDC-101988−101991) may be obtained free of charge on application to CCDC, 12 Union Road, Cambridge CB2 1EZ, UK (Fax: + 44-1223/336−033, E-mail: deposit@ccdc.cam.ac.uk).

[98201]